The Evaluation of Pediatric Malignancies Using Total-body PET/CT With Half Dose ^{18}F-FDG

Wan-Qi Chen
Sun Yat-Sen University Cancer Prevention and Treatment Center: Sun Yat-sen University Cancer Center
Lei Liu
Sun Yat-Sen University Cancer Prevention and Treatment Center: Sun Yat-sen University Cancer Center
Ying-He Li
Sun Yat-Sen University Cancer Prevention and Treatment Center: Sun Yat-sen University Cancer Center
Sha-Tong Li
Sun Yat-Sen University Cancer Prevention and Treatment Center: Sun Yat-sen University Cancer Center
Zhi-Jian Li
Sun Yat-Sen University Cancer Prevention and Treatment Center: Sun Yat-sen University Cancer Center
Wei-Guang Zhang
Sun Yat-Sen University Cancer Prevention and Treatment Center: Sun Yat-sen University Cancer Center
Xu Zhang
Sun Yat-Sen University Cancer Prevention and Treatment Center: Sun Yat-sen University Cancer Center
De-bin Hu
Central Research Institute
Hong-Yan Sun
Central Research Institute
Yun Zhou
Central Research Institute
Wei Fan
Sun Yat-Sen University Cancer Prevention and Treatment Center: Sun Yat-sen University Cancer Center
Yu-mo Zhao
Sun Yat-Sen University Cancer Prevention and Treatment Center: Sun Yat-sen University Cancer Center
Yi-Zhuo Zhang
Sun Yat-Sen University Cancer Prevention and Treatment Center: Sun Yat-sen University Cancer Center
Ying-Ying Hu (huyy@sysucc.org.cn)
Sun Yat-Sen University Cancer Prevention and Treatment Center: Sun Yat-sen University Cancer Center

Research Article

Keywords: Pediatric, Total-body PET/CT, 18F-FDG, Low-dose

Posted Date: March 22nd, 2022

DOI: https://doi.org/10.21203/rs.3.rs-1444072/v1

Abstract

Purpose

To explore the effect of half ^{18}F-FDG dose on image quality of pediatric oncological patients using total-body PET/CT. and investigate the ultra-low dose of administered tracer activity.

Methods

100 pediatric oncological patients who underwent total-body PET/CT using the uEXPLORER scanner with half ^{18}F-FDG dose (1.85 MBq/kg) were retrospectively enrolled. The PET images were firstly reconstructed using all the 600s data, and then split into 300s, 180s, 60s, 40s and 20s duration groups. The subjective analysis method was assessed using a 5-point Likert scales. Objective quantitative metrics included the maximum standard uptake value (SUV_{max}), SUV_{mean}, standard deviation (SD), signal to noise ratio (SNR) and SNR_{norm} of the backgrounds. The variability in lesion SUV_{mean}, SUV_{max}, and tumor-to-background ratio (TBR) were also calculated.

Results

The overall image quality scores in Group 600s, 300s, 180s and 60s were 4.9 ± 0.2, 4.9 ± 0.3, 4.4±0.5 and 3.5±0.5 respectively. All the lesions identified in half-dose images were localised down to G60s (1/20-dose) images; while 56% of the lesion could be clearly identified in G20s (1/60-dose) images. With stimulated reduced doses, SUV_{max} and SD of backgrounds were gradually increased, while TBR values showed no statistically significant deviation among all the groups (all $p > 0.1$). Using the half-dose images as reference, the variability of lesion SUV_{max} gradually increased from G180s to G20s, while lesion SUVmean remained stable for all the age groups. SNR_{norm} was highly correlated with the age in a negative direction.

Conclusions

The total-body PET/CT with half ^{18}F-FDG dose achieved good performance in pediatric patients considering the sufficient image quality and lesion conspicuity. Sufficient image quality and lesion conspicuity could be maintained with an administered dose reduced down to 1/20-dose (0.185 MBq/kg, , estimated effective dose: 0.18–0.26 mSv).

Introduction

Positron emission tomography computed tomography (PET/CT) plays an important role in tumor staging, restaging, and therapy response assessment [1, 2], with demonstrated improved sensitivities and specificities compared with other standard staging procedures [3-5]. However, performing PET/CT in pediatric patients poses unique challenges because children may be more vulnerable to potential carcinogenic effects of ionizing radiation and have a higher sensitivity to developing radiation-induced malignancies [6-8]. Given these concerns, it remains prudent to eliminate unnecessary radiation exposure

by investigating the optimal low-dose radiotracer activity while maintaining high diagnostic efficacy in pediatric malignancies.

Defining the standard low-dose imaging protocols is a difficult task in general due to the large performance difference among PET instruments [9]. Major imaging societies have proposed that the radiotracer dose regimen for pediatric 18-fluoro-2-deoxyglucose (^{18}F-FDG) PET, should be in a range of 3.5–5.3 MBq/kg [10-12]. With the development of the total PET/CT scanner with 194-cm-long axial FOV [13,14], the investigation of further reduce acquisition duration or injected activity can be performed for pediatric patients. several previous studies using reconstruction algorithms to simulate low-dose PET/CT images have shown that pediatric PET tracers can be reduced to 1.5-1.8 MBq/kg [15, 16]. Our preliminary study truncated the acquired full-time total-body PET data to stimulate reconstructed low-dose images, and the results showed that the administered dose of 18F-FDG in pediatric patients could be reduced to 0.3-0.5 mSv, suggesting an optimized regimen of 0.37 MBq/kg for 10 min/bed [17].

However, previous pediatric PET studies were only theoretical extension and to the best of our knowledge, there were few studies about PET/CT with true low-dose injection activity, while the majority of them were limited to adults [18, 19]. In particular, the investigation into the optimal radiotracer activity is even critical to infants and young children. Therefore, we aimed to evaluate the impact of radiotracer dose regimen on image quality and lesion detectability in realistic low dose pediatric PET imaging.

Our study covered an age range from 1 to 13 years old. Total-body PET/CT imaging with half ^{18}F-FDG dose (1.85 MBq/kg) in different pediatric malignancies were retrospectively studied and clinical evidences were provided to assess for the diagnostic efficacy. Meanwhile, the investigation of the ultra-low-dose radiotracer activity was also performed by truncating the list-mode PET data.

Methods

Patients

Pediatric patients who underwent total-body PET/CT using the uEXPLORER scanner (United Imaging Healthcare, Shanghai, China) with half^{18}F-FDG dose (1.85 MBq/kg) for staging or response assessments at Sun Yat-Sen University Cancer Center were retrospectively enrolled from May 2021 to December 2021. All patients were confirmed by postoperative pathologic examination or biopsy.

The inclusion criteria were as follows: (1) under 18 years old, (2) the actual injection regimen should be in a range of 1.7–2.0 MBq/kg. The exclusion criteria were as follows: (1) waiting time after ^{18}F-FDG injection ≥80 min, (2) the body mass above the standard definition of children overweight and obesity [21, 22]. (3) inhomogeneous background uptake, particularly due to liver or spleen metastasis or other irregularities. The study was approved by the Institutional Review Board of Sun Yat-Sen University Cancer Center, and informed consent was obtained from all patients' legal guardians.

Imaging protocol

All patients received ^{18}F-FDG administration after fasting for 4-5 h. List-mode PET data were acquired for 600s after 60±20 min ^{18}F-FDG injection (1.85±0.15 MBq/kg [0.05±0.01 mCi/kg] activity per body weight) using on a 194-cm-long axial FOV total-body PET/CT scanner (uEXPLORER, United Imaging Healthcare, Shanghai, China). Low-dose CT scans with various tube current-time product (25 to 50 mAs) determined by age and body mass were obtained and reconstructed for PET attenuation correction and diagnostic purpose.

Image reconstruction

The full-time raw PET data (600 s acquisition time), as well as the truncated data (300s, 180s, 60s, 40s and 20s), were reconstructed using the ordered subset expectation maximization (OSEM) algorithm incorporating time-of-flight and point-spread function modeling (TOF-PSF) on a medical image processing workstation (uWS-MI, United Imaging Healthcare). All PET/CT images were reconstructed with a matrix of 256×256 and a slice thickness of 2.89 mm, producing 673 image planes per scan and resulting in a voxel size of 2.34×2.34×2.89 mm^3.

Image analysis

Objective analysis Objective image quality evaluation was performed by an experienced technician under the supervision of a radiologist After a review of all pediatric oncologic patients imaged with ^{18}F-FDG PET, different backgrounds (liver, spleen and mediastinum) were selected because of the variability in lesions and organs' uptake pattern, which can provide better contrast and detectability for lesions at various positions. The 2D circular region of interest (ROI) with diameters of 1.5 cm, 2.0cm and 2.0cm, were drawn on a visually homogeneous area of the right liver lobe, the spleen and in the ascending aorta as the mediastinum. The location of FDG-avid lesions was confirmed on CT and PET/CT fusion images, and the ROI was drawn on the plane where the diameter of the lesion was maximal. A bookmark containing the location of the ROI delineated on the 600s image was then propagated to the –truncated acquisition group images using a self-developed software in MATLAB (MathWorks, MA, USA).

Semiquantitative standard uptake value (SUV) parameters, SUV_{max}, SUV_{mean}, and standard deviation (SD) have already been described [20]. Different values of the liver, the spleen and blood pool were calculated. The SNR was calculated via dividing the SUVmean by the SD. The SNR_{norm} was normalized for body weight [23, 24]. The variability in lesion, SUV_{mean}, SUV_{max} and tumor-to-background ratio (TBR) were also calculated. The full-time PET images were served as the reference for other duration groups to evaluate lesion detectability.

Subjective evaluation

For more comprehensive evaluation of low-dose imaging, we use a combination of subjective scoring to assess image quality and lesion detectability performance. Image evaluations were blinded performed by 2 senior nuclear radiologists using the uWS-MI (United Imaging Healthcare, SH, China). Full-count OSEM reconstructions were acquired for 600s served as a quality reference. Low-dose non-contrast CT

reconstruction was served as an anatomic reference. A 5-point Likert scale was used to assess image quality considering the following parameters: (1) noise level, (2) conspicuity of suspected malignant lesions, (3) conspicuity of the liver and spleen margin, and (4) conspicuity of the bone margin. The visual scale for image quality was comprised grades 5 to 1 (Supplementary Table1). Grade 3 indicated the quality of daily routine clinical images obtained with a conventional PET/CT scanner in our center, where PET/CT scans were performed with integrated PET/CT scanner (Biograph mCT, Siemens Healthcare, Henkestr, Germany) with an axial FOV of 16.4 cm (acquisition time 1.5–2.0 min/bed positions 6–10 bp/patient). Image data were acquired 60 ± 10 min after the 18F-FDG injection (3.7 ± 0.37 MBq [0.1mCi]/kg body weight).

All statistical analyses were conducted using the SPSS 22.0 statistical analysis software (IBM, Armonk, NY, USA). The Kruskal-Wallis rank-sum test and Dunn's *post hoc* test for multiple comparisons were applied in subjective image quality analyses between different subsets. The Mann-Whitney U tests was used to compare the quantitative measurements between different groups. Statistical significance was set at two-tailed P <.05.

Results

Patients characteristics

A total of one-hundred pediatric patients (33 females and 67 males; mean age: 7.9 years; range: 1–13 years) with different tumors were included in this study. The characteristics of the patients were summarized in Table 1. The most prevalent diseases included lymphoma (n=38), rhabdomyosarcoma (n=35), neuroblastoma (n=15), and Langerhans cell histiocytosis (n=3) respectively. Twenty-four patients of newly diagnosed cancer underwent PET/CT for an initial assessment (lesion detection and staging), while others underwent PET/CT for recurrence detection (restaging) and therapy response assessment. A total of 70 detectable lesions were included.

Subjective assessment of image quality

The subjective image quality assessed by 5-point Likert scale were summarized in Table 2. The mean and SD of the image quality scores in G600s were 4.9 ± 0.2 for overall quality, 5.0 ± 0.0 for lesion conspicuity and 4.9 ± 0.3 for image noise, which demonstrated that half-dose pediatric PET imaging can meet the diagnostic requirement. The overall image quality scores for G300s, G180s and G60s were 4.9 ± 0.2, 4.9 ± 0.3, 4.4±0.5 and 3.5±0.5 points, respectively. All G60s images were clinical acceptable (≥3 points), while 13 % and 83% of low-dose images were subsequent graded as 1 and 2 on the G40s and G20s images. Image quality scores in G20s (2.0 ± 0.5) were significantly lower than other groups (all p□0.05). As shown in Fig 1, 95% cases in G600s and 87% cases in G300s were evaluated as 5 points. The frequency of an overall image quality score evaluated as 5 points was decreased from G600s to G20s, while the noise level showed an opposite tendency. The image noise was more deranged than the overall quality and lesion conspicuity.

Lesion detectability

As shown in Fig 1, 100% of the lesions identified in half-dose images were localized even down to G60s images; while 92% and 56% of the lesions could be clearly identified in G40s (1/30-dose) and G20s (1/60-dose) images, respectively

Quantitative measurement of image quality

The Comparison of quantitative image quality metrics in the total-body PET/CT among G600s to G20s images was shown in Fig 2. The SUVs of lesions and background were measured to assess the change as the dose was reduced. Both SUV_{max} and SD were plotted using the average of multiple VOI measurements, with an error bar. As shown in Table 3, in full-time acquired PET/CT for 600s, the liver SUV_{max} and liver SD were 1.88±0.43 and 0.09±0.03, which were significantly lower than those in other short acquisition groups (all $p < 0.05$). Additionally, the SUV_{max} and SD of the spleen and mediastinum were showed the same tendency. With reduced doses from the half-dose (1.85MBq/kg) in pediatric patients, SUV_{max} and SD of backgrounds were gradually increased, while the TBR values were almost the same as shown in Fig. 2D. There was no statistically significant deviation among all the groups regarding the TBR values no matter which organ was used as contrast (all $p > 0.1$). Considering the known change 18F-FDG uptake with age [23], three age subgroups were used. The scatterplots of the SNR and SNR_{norm} was shown in Fig 3. In pediatric patients, all SNR was showed no correlation with age. In contrast, SNR_{norm} was strongly correlated with age in a negative direction (respectively, liver r=-.571, spleen r=-.643, mediastinum r= -.651, all $p<0.001$).

The bias and variability in lesion SUV measurement

Lesion SUV measurements was shown in Fig 4. Using half-dose images as reference, G300s (1/4-dose) showed good consistency in lesion detection. Changes in lesion SUV_{max} had a maximum average bias of approximately 8% for G20s (1/60dose) of pediatric patients from age of 4-6 years old. Except the G20s, the average bias on lesion SUV_{max} was negative from almost all other age groups. As the acquisition time was reduced from 180s to 20s, there was a progressive increase in the variability of lesion SUV_{max} for all age groups, with notable significance in G20s (all $p<0.05$). Comparatively, the bias and variability in lesion SUV_{mean} uptake remained to be low as the scanning time was reduced in all age groups, with no significance (all $p > 0.1$).

Discussion

PET/CT provides both the anatomic and metabolic features of malignant tumors for clinical evaluation, which was also demonstrated to be more sensitive particularly in detecting lymph node, bone marrow involvement and distant recurrent metastases than CT alone [26, 27]. The cumulative ionizing radiation dose by repeated scans continues to be concern, although the relationship between exposure and radiation-related illness remains debatable [4]. Protocols for low-dose ^{18}F-FDG PET/CT by the influential

imaging associations have been posted, involving the reduction of radiotracer activity and shortening of the acquisition time. Meanwhile, several studies have focused on investigation of the effectivity of the ultra-low-dose PET imaging. Work from Liu et al. [18] has shown the total-body dynamic ^{18}F-FDG PET imaging 10× reduction of injected activity (0.37 MBq/kg) allows equal performance to full-activity PET imaging in healthy volunteers. Shi et al .[19] found that the total-body PET/CT with half-dose ^{18}F-FDG activity can achieve the comparable image quality to conventional PET/CT.

However, pediatric patients are at a higher risk of radiation-induced cancers due to their developing bodies and greater life expectancies [28, 29]. In addition, the reported sensitivities and specificities of ^{18}F-FDG PET/CT for tumor staging in children are over 90% [30, 31]. Few studies were concentrated on PET/CT low-dose injection activity in pediatric patients, while most of the them were only theoretical [15, 16]. Our study is the first to evaluate the impact of radiotracer dose regimen in realistic low-dose pediatric PET imaging data in the larger sample size.

The image quality of PET/CT is affected by multiple factors including the various instruments, imaging agents, waiting time, reconstruction parameters, individual subject factors (including age, BMI, blood glucose level, disease history, etc.) [25, 32, 33]. In order to eliminate the deviations as little as possible, we set a relatively narrow subject inclusion criteria, excluding children with excessive waiting time, true injected dose and BMI. Our results from the realistic half-dose and low-dose images covered an age range from 1 to 13 years old.

The disease referred to the specific common pediatric malignancies, mainly lymphomas, sarcomas, and neuroblastoma. Pediatric patients in various clinical stages were all involved (including newly diagnosed cancer for an initial staging, restaging and therapy response assessment). Different backgrounds (liver, spleen and blood pool) were selected for thoroughly evaluation considering the variability in lesions and organs' uptake pattern, where the mediastinal blood pool, liver, and spleen serve as the cutoffs for PET positivity in the evaluation of the response assessment and post-treatment surveillance [34-37]. However, VOI determination could be still difficult due to the large difference in children's age, height and weight.

Our results have shown that the total-body PET/CT with half-dose (1.85 MBq/kg, estimated effective dose: 1.76–2.57 mSv) of ^{18}F-FDG was feasible for clinical application in pediatric patients, which was much lower than previous initiatives. The mean and SD of the image quality scores in G600s were 4.9 ± 0.2 for overall quality, 5.0 ± 0.0 for lesion conspicuity and 4.9 ± 0.3 for image noise. The image quality and lesion detectability were performed well as the dose of radiation reduced. In terms of the acquisition time, a longer time always results in higher image quality. The image quality showed a slight degradation as the dosing regimen reduced in low-dose images from G600s (1/2-dose) to G20s (1/60-dose) based on the Likert scoring. While the degradation in noise level was more obvious. Taking the G600s image as a reference, image quality scores in G20s were significantly lower. Based on the clinical data, we revised our original theoretical estimations [16] and proposed updated recommended injection-dose and acquisition time (Supplementary Table 2). Safe and sufficient overall image quality and lesion conspicuity available for clinical use could be maintained down to G60s (0.185 MBq/kg, estimated effective dose: 0.18–0.26

mSv), none of half-dose images was rated as undiagnostic, which was even beyond our previous estimation. For patients needs multiple PET/CT scan for therapy response assessment, lower-dose PET was recommended to manage the over-all exposure, while ultra-fast-scan with a full or half dose was recommended for patients that intolerant of long scan duration.

The change in lesion detectability with dose level was comparatively minimal. Fig 5 showed a representative view of a PET examination reconstructed using OSEM. As expected, lower-dose images appeared to be nosier because of the reduced number of events in the PET list file. The overall image quality scores were typically evaluated as 5, 5, 4, 3, 3 and 2 points, respectively, for G600s to G20s. The lesion was even clearly identifiable reduced down to 1/60-dose. However, our results showed that even some small lesions with low SUV uptake became difficult to detect in low-dose images due to the increased noise of background. There were 8% and 44% of false-negative lesions which could not be clearly demonstrated in G40s (1/30-dose) and G20s (1/60-dose) images, respectively, indicating they may be not feasible for clinical diagnose and therapy response assessment.

Consistent with previous observation [19, 38], the objective analyses showed that there was a pronounced increase in SUV_{max} and SD of backgrounds as the simulated dose was reduced, which was consistent with the visible increase noise in PET images at low doses and previous research [38, 39]. The same tendency was demonstrated in all three backgrounds, which means that a shortened acquisition time might diminish the accuracy of the SUV measurement. This increase may be caused by noise amplification therefore causing the maximum pixel value to be higher in the background measurement. There was no statistically significant deviation in TBR values as the dose level systematically reduced from half-dose, which further indicated a good maintain in lesion conspicuity.

One of major challenges in the pediatrics low-dose PET/CT images is the large variation in patient's age, range from infants, children and adolescents with different size and metabolism, which impacts the dosimetry measurement [40, 41]. The increase in ^{18}F-FDG uptake may be caused by age related changes in body mass, blood volume, organ volume and function [34, 42]. Separate evaluations are warranted for multiple pediatric age groups. Our studies are based on PET imaging data from patients with age ranging from 1 to 13 years old, especially involving infants, which were more distinct from adults, therefore directly including the age-dependent pharmacokinetics of ^{18}F-FDG. SNR has almost no correlation with age, which means that, the currently half-dose regimen already provided a constant image quality throughout our patient population. Smaller children showed high SNR_{norm} values, which was probably caused by less attenuation and scatter due to smaller body mass. The results indicated that for the younger patients, the less activity is needed to obtain optimal image quality, which means the dosage regimen can be further reduced in younger patients, somehow alleviating the concern of repeated PET/CT.

As shown in Fig 4, G300s (1/4-dose) showed that high consistency in both lesion SUV_{max} and SUV_{mean} was observed compared to half-dose images. The variability in lesion SUV_{max} gradually increased as the dose reduced, generally lower than 20%, which was similar to previous studies [43, 44]. The average bias on lesion SUV_{max} was negative from almost all other age groups except G20s (1/60-dose), which was

probably due to the higher noise in G20s. This observation also indicated unstable values of lesion SUV_{max} at low-dose images. Comparatively, lesion SUV_{mean} showed a smaller bias and variability as dose levels were reduced, which suggested that SUV_{mean} was a much more accurate and stable metric for image quality at lower dose.

Our study had several potential limitations. First, it was a single-centre study, and ^{18}F-FDG PET/CT images were obtained relevant to only a specific scanner, therefore it may not be generalizable to other centers, other PET equipment or tracers beyond FDG. Secondly, pediatric patients in our center were mainly restricted to several specific common malignancies such as lymphomas, sarcomas and neuroblastoma. The small variety of tumors might have resulted in selection bias. Furthermore, we did not used the disease as a subgroup because of the relatively small population of each tumor and different disease stages.

Conclusions

Our study demonstrated that total-body PET/CT using true half-dose of ^{18}F-FDG can meet the needs of clinical diagnose. Besides, sufficient image quality and lesion conspicuity could be achieved at a relatively even lower tracer dose to 1/20-dose (0.185 MBq/kg, estimated effective dose: 0.18–0.26 mSv). This optimization will serve as a novel reference to further pediatric PET dose investigation and lead to more efficient PET/CT while maintaining its high clinical value.

Declarations

Funding: The authors did not receive financial support from any organization for the submitted work.

Conflicts of interest/Competing interests: Author Hong-Yan Sun, De-Bin Hu and Yun-Zhou are employees of United Imaging Research. The other authors working at Sun-Yat Sen University Cancer Center have full control of the data and declare that they have no conflict of interest.

Availability of data and material: The datasets generated during and/or analysed during the current study are available from the corresponding author on reasonable request.

Code availability: The code applied during and/or analysed during the current study are available from the corresponding author on reasonable request.

Authors' contributions: Conceptualization: Ying-Ying Hu, Yi-Zhuo Zhang, Yu-Mo Zhao; Methodology: Wan-Qi Chen, Lei Liu, Yu-Mo Zhao, Zhi-Jian Li; Formal analysis and investigation: Ying-Ying Hu, Wanqi-Chen, Lei Liu, Zhi-Jian Li, Wei-Guang Zhang; Writing - original draft preparation: Wanqi-Chen, Lei Liu, Ying-Ying Hu; Writing - review and editing: Ying-ying Hu, Yi-Zhuo Zhang, Yu-Mo Zhao, Ying-He Li, Sha-tong Li, Xu Zhang; Technical support: Hong-Yan Sun, De-Bin Hu, Yun-Zhou; Resources: Ying-ying Hu. Supervision: Yu-Mo Zhao, Yi-Zhuo Zhang, Ying-Ying Hu. All authors read and approved the final manuscript.

Ethics approval: All procedures performed in studies involving human participants were in accordance with the ethical standards of the institutional and/or national research committee and with the 1964 Helsinki declaration and its later amendments or comparable ethical standards.

Consent to participate: Informed consent was obtained from legal guardians.

Consent for publication: Additional informed consent was obtained from all legal guardians for whom identifying information is included in this article.

References

1. Boellaard R D-BR, Oyen WJ, Giammarile F, Tatsch K, Eschner W, et al. European Association of Nuclear Medicine (EANM). FDG PET/CT: EANM procedure guidelines for tumour imaging: version 2.0. Eur J Nucl Med Mol Imaging 2015;42: 28-54. doi:10.1007/s00259-014-2961-x.
2. Fahey FH TS, Adelstein SJ. . Minimizing and communicating radiation risk in pediatric nuclear medicine. 2011 J Nucl Med 2011; Aug;52:1240-51. doi:10.2967/jnumed.109.069609.
3. Ricard F, Cimarelli S, Deshayes E, Mognetti T, Thiesse P, Giammarile F. Additional Benefit of F-18 FDG PET/CT in the staging and follow-up of pediatric rhabdomyosarcoma. Clinical nuclear medicine. 2011;36:672-7. doi:10.1097/RLU.0b013e318217ae2e.
4. Fahey FH, Goodkind A, MacDougall RD, Oberg L, Ziniel SI, Cappock R, et al. Operational and Dosimetric Aspects of Pediatric PET/CT. Journal of nuclear medicine : official publication, Society of Nuclear Medicine. 2017;58:1360-6. doi:10.2967/jnumed.116.182899.
5. Turpin S, Martineau P, Levasseur MA, Meijer I, Décarie JC, Barsalou J, et al. 18F-Flurodeoxyglucose positron emission tomography with computed tomography (FDG PET/CT) findings in children with encephalitis and comparison to conventional imaging. European journal of nuclear medicine and molecular imaging. 2019;46:1309-24. doi:10.1007/s00259-019-04302-x.
6. Chawla SC, Federman N, Zhang D, Nagata K, Nuthakki S, McNitt-Gray M, et al. Estimated cumulative radiation dose from PET/CT in children with malignancies: a 5-year retrospective review. Pediatric radiology. 2010;40:681-6. doi:10.1007/s00247-009-1434-z.
7. Mercolini F, Zucchetta P, Jehanno N, Corradini N, Van Rijn RR, Rogers T, et al. Role of (18)F-FDG-PET/CT in the staging of metastatic rhabdomyosarcoma: a report from the European paediatric Soft tissue sarcoma Study Group. European journal of cancer (Oxford, England : 1990). 2021;155:155-62. doi:10.1016/j.ejca.2021.07.006.
8. Nievelstein RA, Quarles van Ufford HM, Kwee TC, Bierings MB, Ludwig I, Beek FJ, et al. Radiation exposure and mortality risk from CT and PET imaging of patients with malignant lymphoma. European radiology. 2012;22:1946-54. doi:10.1007/s00330-012-2447-9.
9. Alessio AM, Farrell MB, Fahey FH. Role of Reference Levels in Nuclear Medicine: A Report of the SNMMI Dose Optimization Task Force. Journal of nuclear medicine : official publication, Society of Nuclear Medicine. 2015;56:1960-4. doi:10.2967/jnumed.115.160861.

10. Poli GL, Torres L, Coca M, Veselinovic M, Lassmann M, Delis H, et al. Paediatric nuclear medicine practice: an international survey by the IAEA. European journal of nuclear medicine and molecular imaging. 2020;47:1552-63. doi:10.1007/s00259-019-04624-w.
11. Treves ST, Gelfand MJ, Fahey FH, Parisi MT. 2016 Update of the North American Consensus Guidelines for Pediatric Administered Radiopharmaceutical Activities. Journal of nuclear medicine : official publication, Society of Nuclear Medicine. 2016;57:15n-8n.
12. Lassmann M, Biassoni L, Monsieurs M, Franzius C. The new EANM paediatric dosage card: additional notes with respect to F-18. European journal of nuclear medicine and molecular imaging. 2008;35:1666-8. doi:10.1007/s00259-008-0799-9.
13. Cherry SR, Jones T, Karp JS, Qi J, Moses WW, Badawi RD. Total-Body PET: Maximizing Sensitivity to Create New Opportunities for Clinical Research and Patient Care. Journal of nuclear medicine : official publication, Society of Nuclear Medicine. 2018;59:3-12. doi:10.2967/jnumed.116.184028.
14. Badawi RD, Shi H, Hu P, Chen S, Xu T, Price PM, et al. First Human Imaging Studies with the EXPLORER Total-Body PET Scanner. Journal of nuclear medicine : official publication, Society of Nuclear Medicine. 2019;60:299-303. doi:10.2967/jnumed.119.226498.
15. Schmall JP, Surti S, Otero HJ, Servaes S, Karp JS, States LJ. Investigating Low-Dose Image Quality in Whole-Body Pediatric (18)F-FDG Scans Using Time-of-Flight PET/MRI. Journal of nuclear medicine : official publication, Society of Nuclear Medicine. 2021;62:123-30. doi:10.2967/jnumed.119.240127.
16. Gatidis S, Schmidt H, la Fougère C, Nikolaou K, Schwenzer NF, Schäfer JF. Defining optimal tracer activities in pediatric oncologic whole-body (18)F-FDG-PET/MRI. European journal of nuclear medicine and molecular imaging. 2016;43:2283-9. doi:10.1007/s00259-016-3503-5.
17. Zhao YM, Li YH, Chen T, Zhang WG, Wang LH, Feng J, et al. Image quality and lesion detectability in low-dose pediatric (18)F-FDG scans using total-body PET/CT. European journal of nuclear medicine and molecular imaging. 2021;48:3378-85. doi:10.1007/s00259-021-05304-4.
18. Liu G, Hu P, Yu H, Tan H, Zhang Y, Yin H, et al. Ultra-low-activity total-body dynamic PET imaging allows equal performance to full-activity PET imaging for investigating kinetic metrics of (18)F-FDG in healthy volunteers. European journal of nuclear medicine and molecular imaging. 2021;48:2373-83. doi:10.1007/s00259-020-05173-3.
19. Tan H, Sui X, Yin H, Yu H, Gu Y, Chen S, et al. Total-body PET/CT using half-dose FDG and compared with conventional PET/CT using full-dose FDG in lung cancer. European journal of nuclear medicine and molecular imaging. 2021;48:1966-75. doi:10.1007/s00259-020-05091-4.
20. El Fakhri G, Surti S, Trott CM, Scheuermann J, Karp JS. Improvement in lesion detection with whole-body oncologic time-of-flight PET. Journal of nuclear medicine : official publication, Society of Nuclear Medicine. 2011;52:347-53. doi:10.2967/jnumed.110.080382.
21. Spinelli A, Buoncristiano M, Nardone P, Starc G, Hejgaard T, Júlíusson PB, et al. Thinness, overweight, and obesity in 6- to 9-year-old children from 36 countries: The World Health Organization European Childhood Obesity Surveillance Initiative-COSI 2015-2017. Obesity reviews : an official journal of the International Association for the Study of Obesity. 2021;22 Suppl 6:e13214. doi:10.1111/obr.13214.

22. Daniels SR, Arnett DK, Eckel RH, Gidding SS, Hayman LL, Kumanyika S, et al. Overweight in children and adolescents: pathophysiology, consequences, prevention, and treatment. Circulation. 2005;111:1999-2012. doi:10.1161/01.Cir.0000161369.71722.10.
23. de Groot EH, Post N, Boellaard R, Wagenaar NR, Willemsen AT, van Dalen JA. Optimized dose regimen for whole-body FDG-PET imaging. EJNMMI research. 2013;3:63. doi:10.1186/2191-219x-3-63.
24. Cox CPW, van Assema DME, Verburg FA, Brabander T, Konijnenberg M, Segbers M. A dedicated paediatric [(18)F]FDG PET/CT dosage regimen. EJNMMI research. 2021;11:65. doi:10.1186/s13550-021-00812-8.
25. Meier JM, Alavi A, Iruvuri S, Alzeair S, Parker R, Houseni M, et al. Assessment of age-related changes in abdominal organ structure and function with computed tomography and positron emission tomography. Seminars in nuclear medicine. 2007;37:154-72. doi:10.1053/j.semnuclmed.2007.02.001.
26. Wegner EA, Barrington SF, Kingston JE, Robinson RO, Ferner RE, Taj M, et al. The impact of PET scanning on management of paediatric oncology patients. European journal of nuclear medicine and molecular imaging. 2005;32:23-30. doi:10.1007/s00259-004-1645-3.
27. Montravers F, McNamara D, Landman-Parker J, Grahek D, Kerrou K, Younsi N, et al. [(18)F]FDG in childhood lymphoma: clinical utility and impact on management. European journal of nuclear medicine and molecular imaging. 2002;29:1155-65. doi:10.1007/s00259-002-0861-y.
28. Sgouros G, Frey EC, Bolch WE, Wayson MB, Abadia AF, Treves ST. An approach for balancing diagnostic image quality with cancer risk: application to pediatric diagnostic imaging of 99mTc-dimercaptosuccinic acid. Journal of nuclear medicine : official publication, Society of Nuclear Medicine. 2011;52:1923-9. doi:10.2967/jnumed.111.092221.
29. Alessio AM, Sammer M, Phillips GS, Manchanda V, Mohr BC, Parisi MT. Evaluation of optimal acquisition duration or injected activity for pediatric 18F-FDG PET/CT. Journal of nuclear medicine : official publication, Society of Nuclear Medicine. 2011;52:1028-34. doi:10.2967/jnumed.110.086579.
30. Tatsumi M, Miller JH, Wahl RL. 18F-FDG PET/CT in evaluating non-CNS pediatric malignancies. Journal of nuclear medicine : official publication, Society of Nuclear Medicine. 2007;48:1923-31. doi:10.2967/jnumed.107.044628.
31. Uslu L, Donig J, Link M, Rosenberg J, Quon A, Daldrup-Link HE. Value of 18F-FDG PET and PET/CT for evaluation of pediatric malignancies. Journal of nuclear medicine : official publication, Society of Nuclear Medicine. 2015;56:274-86. doi:10.2967/jnumed.114.146290.
32. Büsing KA, Schönberg SO, Brade J, Wasser K. Impact of blood glucose, diabetes, insulin, and obesity on standardized uptake values in tumors and healthy organs on 18F-FDG PET/CT. Nuclear medicine and biology. 2013;40:206-13. doi:10.1016/j.nucmedbio.2012.10.014.
33. Yeung HW, Sanches A, Squire OD, Macapinlac HA, Larson SM, Erdi YE. Standardized uptake value in pediatric patients: an investigation to determine the optimum measurement parameter. European journal of nuclear medicine and molecular imaging. 2002;29:61-6. doi:10.1007/s00259-001-0662-8.
34. Sastre J, Pallardó FV, Plá R, Pellín A, Juan G, O'Connor JE, et al. Aging of the liver: age-associated mitochondrial damage in intact hepatocytes. Hepatology (Baltimore, Md). 1996;24:1199-205.

doi:10.1002/hep.510240536.

35. Schmidkonz C, Krumbholz M, Atzinger A, Cordes M, Goetz TI, Prante O, et al. Assessment of treatment responses in children and adolescents with Ewing sarcoma with metabolic tumor parameters derived from (18)F-FDG-PET/CT and circulating tumor DNA. European journal of nuclear medicine and molecular imaging. 2020;47:1564-75. doi:10.1007/s00259-019-04649-1.
36. Pijl JP, Kwee TC, Slart R, Yakar D, Wouthuyzen-Bakker M, Glaudemans A. Clinical implications of increased uptake in bone marrow and spleen on FDG-PET in patients with bacteremia. European journal of nuclear medicine and molecular imaging. 2021;48:1467-77. doi:10.1007/s00259-020-05071-8.
37. Patel NH, Osborne MT, Teague H, Parel P, Svirydava M, Sorokin AV, et al. Heightened splenic and bone marrow uptake of (18)F-FDG PET/CT is associated with systemic inflammation and subclinical atherosclerosis by CCTA in psoriasis: An observational study. Atherosclerosis. 2021;339:20-6. doi:10.1016/j.atherosclerosis.2021.11.008.
38. Akamatsu G, Ishikawa K, Mitsumoto K, Taniguchi T, Ohya N, Baba S, et al. Improvement in PET/CT image quality with a combination of point-spread function and time-of-flight in relation to reconstruction parameters. Journal of nuclear medicine : official publication, Society of Nuclear Medicine. 2012;53:1716-22. doi:10.2967/jnumed.112.103861.
39. Zhang YQ, Hu PC, Wu RZ, Gu YS, Chen SG, Yu HJ, et al. The image quality, lesion detectability, and acquisition time of (18)F-FDG total-body PET/CT in oncological patients. European journal of nuclear medicine and molecular imaging. 2020;47:2507-15. doi:10.1007/s00259-020-04823-w.
40. Shammas A, Lim R, Charron M. Pediatric FDG PET/CT: physiologic uptake, normal variants, and benign conditions. Radiographics : a review publication of the Radiological Society of North America, Inc. 2009;29:1467-86. doi:10.1148/rg.295085247.
41. Halpern BS, Dahlbom M, Quon A, Schiepers C, Waldherr C, Silverman DH, et al. Impact of patient weight and emission scan duration on PET/CT image quality and lesion detectability. Journal of nuclear medicine : official publication, Society of Nuclear Medicine. 2004;45:797-801.
42. Accorsi R, Karp JS, Surti S. Improved dose regimen in pediatric PET. Journal of nuclear medicine : official publication, Society of Nuclear Medicine. 2010;51:293-300. doi:10.2967/jnumed.109.066332.
43. de Langen AJ, Vincent A, Velasquez LM, van Tinteren H, Boellaard R, Shankar LK, et al. Repeatability of 18F-FDG uptake measurements in tumors: a metaanalysis. Journal of nuclear medicine : official publication, Society of Nuclear Medicine. 2012;53:701-8. doi:10.2967/jnumed.111.095299.
44. Wahl RL, Jacene H, Kasamon Y, Lodge MA. From RECIST to PERCIST: Evolving Considerations for PET response criteria in solid tumors. Journal of nuclear medicine : official publication, Society of Nuclear Medicine. 2009;50 Suppl 1:122s-50s. doi:10.2967/jnumed.108.057307.

Tables

Table 1. Clinical characteristics of pediatric oncological patients underwent total-body PET/CT with half-dose 18F-FDG activity.

Characteristic	Value (n=100)
Age (years old)	7.9±3.3 (range 1~13)
1~3	9
4~6	28
7~13	63
Sex	
Male	67
Female	33
BMI (kg/m^2)	15.5±2.5
Injected dose (MBq)	51.0±22.3
Injected dose per weight (MBq/kg)	1.85±0.15
Lesion number	70
Pathological type	
Lymphoma	38
Rhabdomyosarcoma	35
Neuroblastoma	15
Langerhans cell histiocytosis	3
Germ cell tumor	2
Other diseases	7

Table 2. Subjective image quality assessed by 5-point Likert scale.

Groups	Overall quality	Lesion conspicuity	Image noise
G600s	4.9 ± 0.2	5.0 ± 0.0	4.9 ± 0.3
G300s	4.9 ± 0.3	5.0 ± 0.0	4.6 ± 0.5
G180s	4.4 ± 0.5	4.9 ± 0.3	4.1 ± 0.3
G60s	3.5 ± 0.5	4.1 ± 0.6	3.2 ± 0.5
G40s	3.0 ± 0.5	3.5 ± 0.8	2.8 ± 0.4
G20s	2.0 ± 0.5	2.6 ± 0.8	1.7 ± 0.5

*All data were presented as Mean ± SD.

Table 3. SUV and SD measurement of backgrounds.

	Group 600s	Group 300s	Group 180s	Group 60s	Group 40s	Group 20s
Liver SUV_{max}	1.87 ± 0.43	1.97 ± 0.45	2.07 ± 0.45	2.42 ± 0.59	2.63 ± 0.61	3.11 ± 0.75
Liver SD	0.09 ± 0.03	0.12 ± 0.03	0.15 ± 0.04	0.25 ± 0.07	0.33 ± 0.09	0.43 ± 0.10
Spleen SUV_{max}	1.57 ± 0.42	1.65 ± 0.45	1.72 ± 0.45	1.97 ± 0.49	2.32 ± 0.61	5.51 ± 0.66
Spleen SD	0.09 ± 0.05	0.12 ± 0.06	0.13 ± 0.05	0.22 ± 0.07	0.30 ± 0.10	0.37± 0.09
Mediastinum SUV_{max}	1.32 ± 0.33	1.37 ± 0.34	1.44 ± 0.36	1.59 ± 0.42	1.67 ± 0.38	2.02 ± 0.60
Mediastinum SD	0.1± 0.05	0.11 ± 0.05	0.13 ± 0.04	0.19 ± 0.07	0.22 ± 0.10	0.30 ± 0.11

*All data were presented as Mean ± SD.

Figures

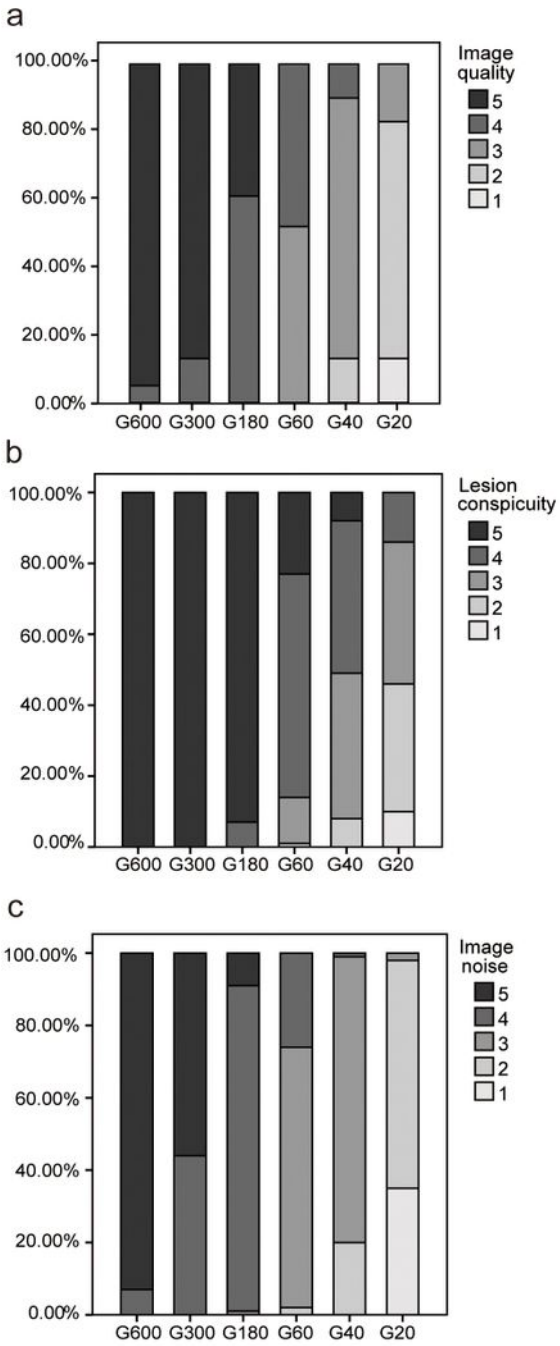

Figure 1

The distribution of subjective three-dimensional image quality scoring among different groups. (A) Overall image quality. (B) Lesion conspicuity. (C) Image noise.

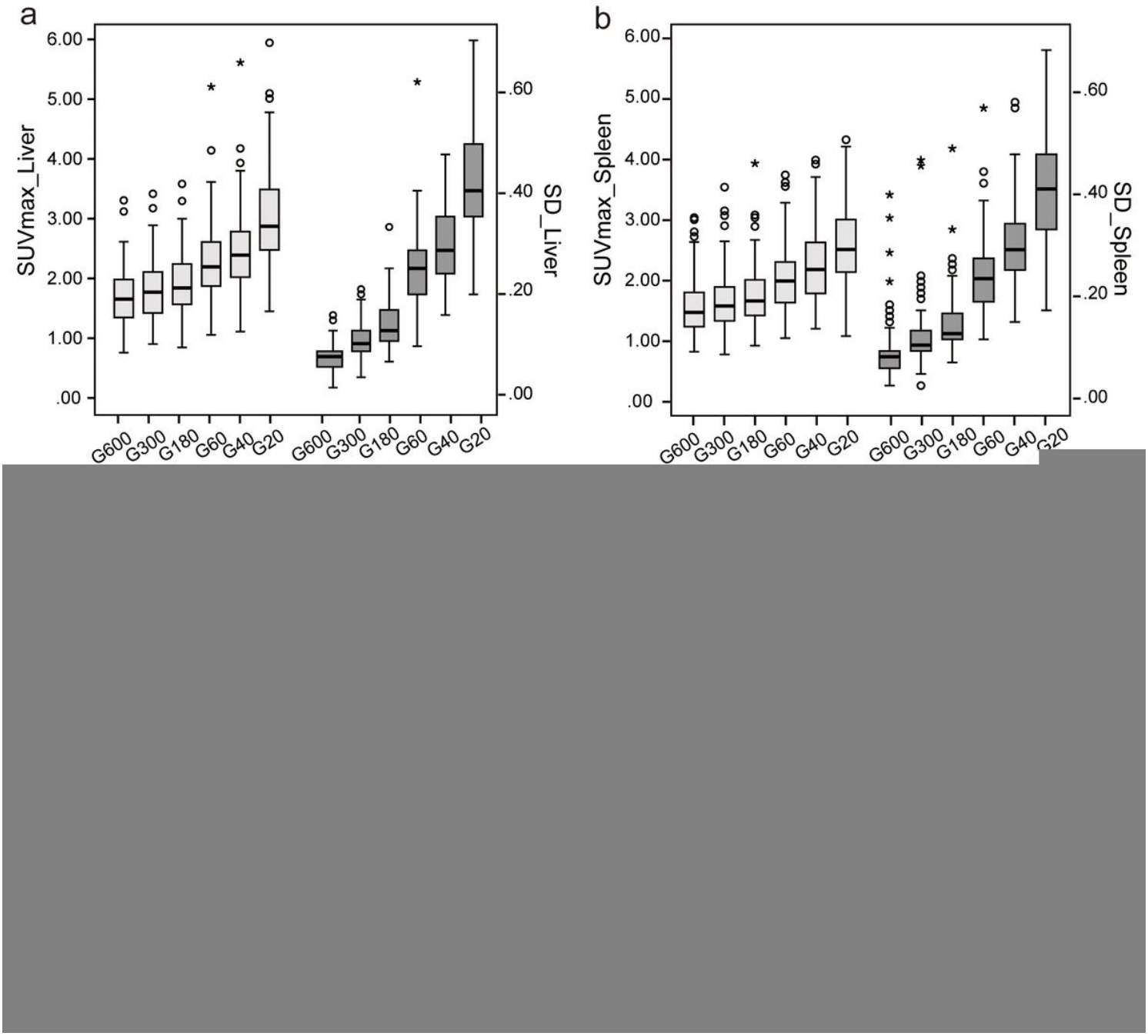

Figure 2

The Comparison of objective image quality parameters in total-body PET/CT among G20s to G600s images. (A) Liver SUV_{max} and SD. (B) Spleen SUV_{max} and SD. (C) Mediastinum SUV_{max} and SD. The SUV_{max} and SD of background parameters increased gradually as the simulated dose was reduced. The differences between each group were statistically significant ($p < 0.05$). (D) The tumor-to-background ratio (TBR) was calculated by dividing the SUV_{max} of the lesion by the SUV_{mean} of the liver, the spleen and blood pool. The TBR values were almost the same. The differences were not statistically significant (all $p > 0.1$).

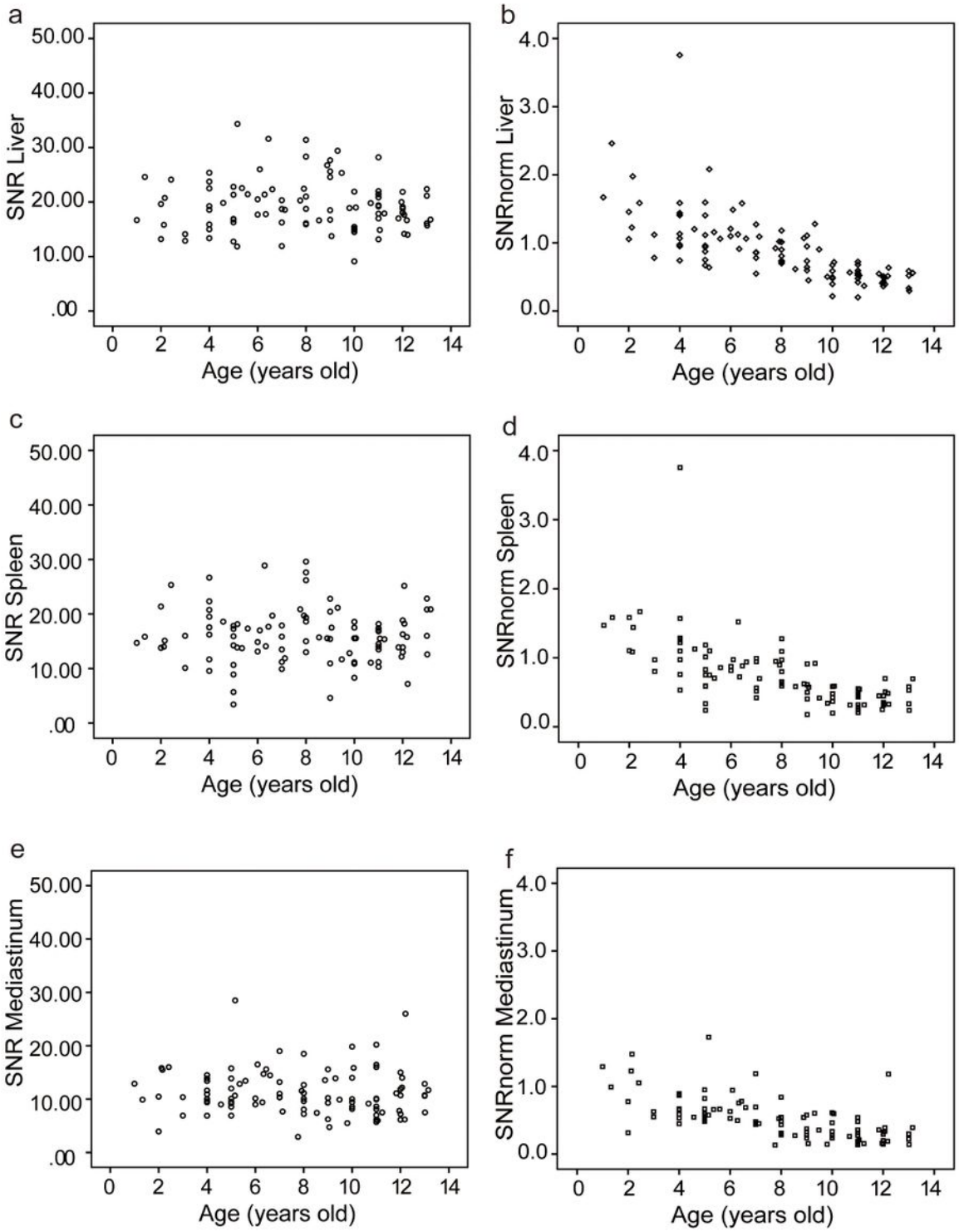

Figure 3

Scatterplots of the SNR liver, spleen, mediastinum (A, C, E) and the SNR_{norm} liver, spleen, mediastinum (B, D, F) against age

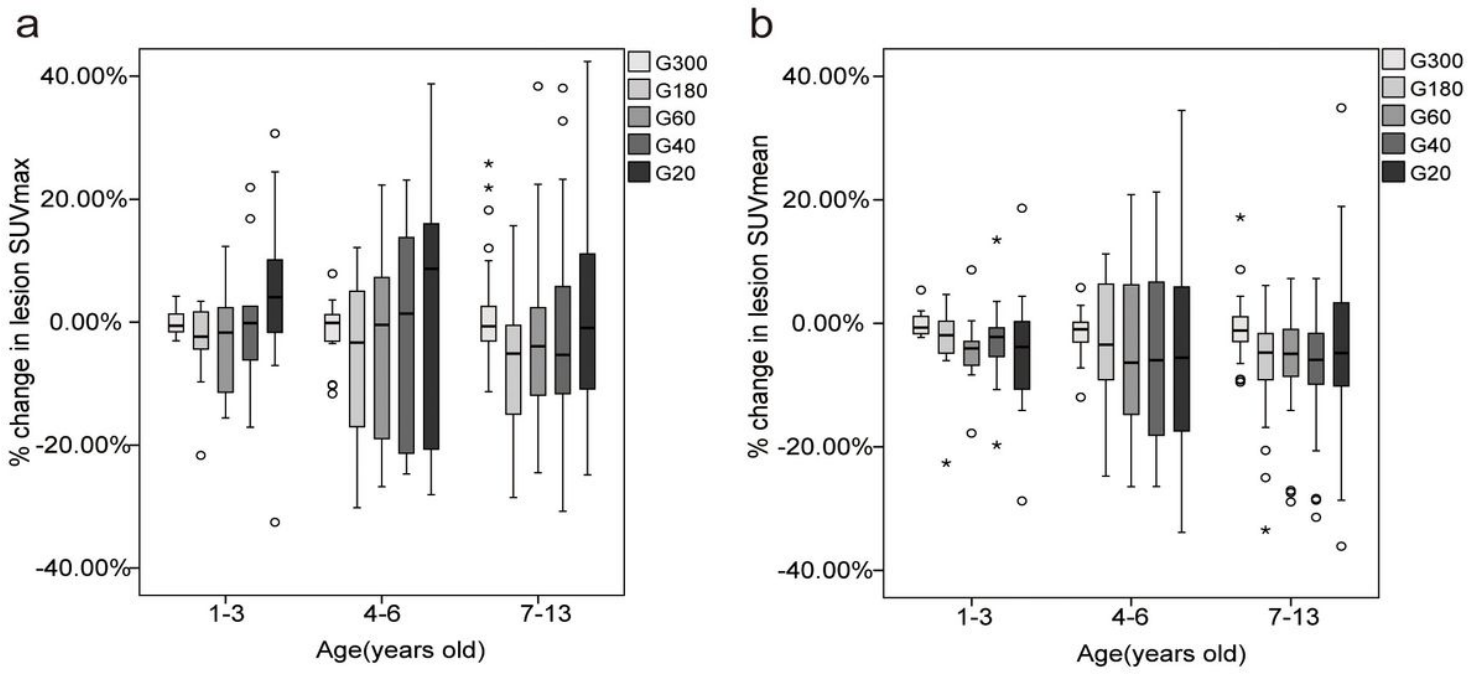

Figure 4

The bias and variability in lesion SUV_{max} (A) and SUV_{mean} (B) at 5 dose levels. Data were divided into three age subgroups. Plot shows the percent changes compared with the half-dose images (G600s). Total lesion count was 70.

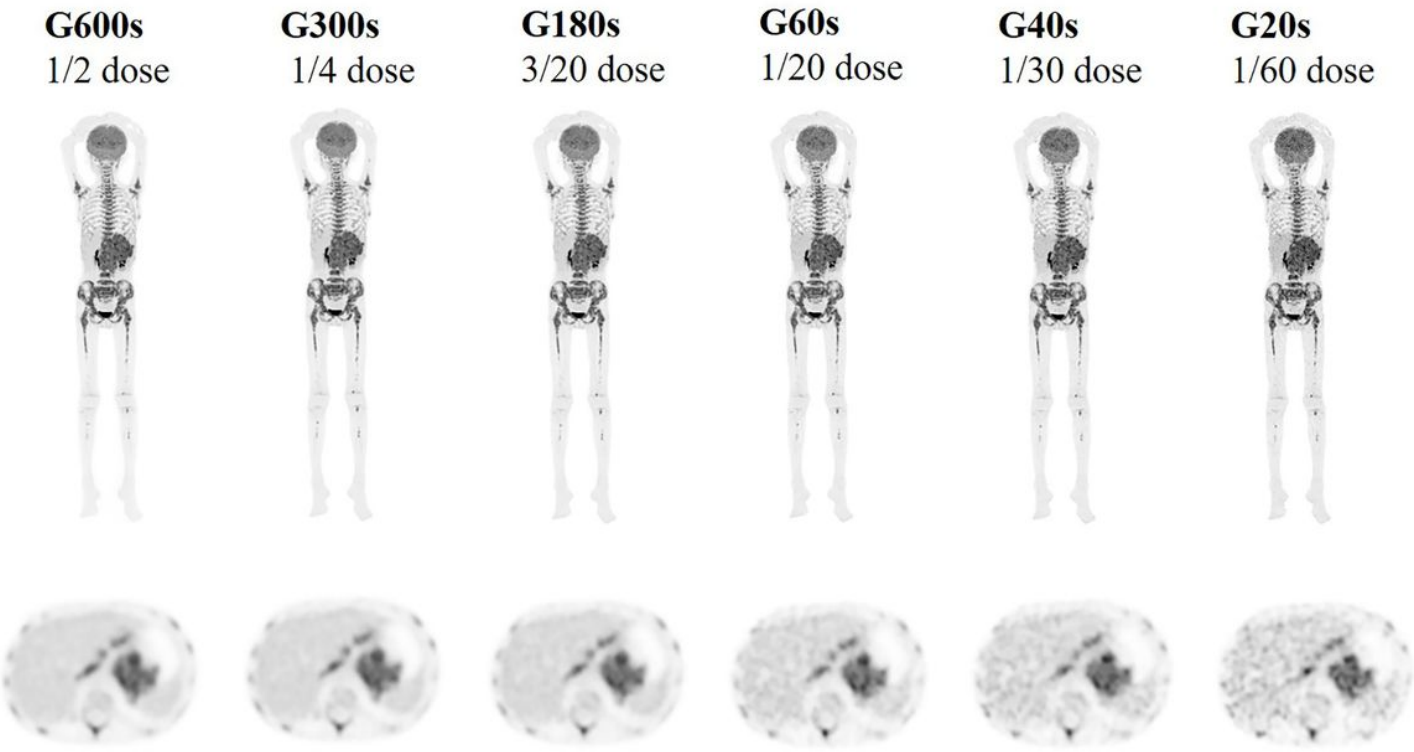

Figure 5

An 11-year-old child with neuroblastoma confirmed by following surgery. The maximum intensity projection (MIP) of the half-dose image and coronal view and axial images of the serial dose reduction image generated by reduced count. The overall image quality scores of G600s to G20s were 5, 5, 4, 3, 3 and 2 points, respectively. The lesion was even identifiable reduced down to 1/60-dose.

Supplementary Files

This is a list of supplementary files associated with this preprint. Click to download.

- SupplementaryTables.docx